Science is a beautiful gift to
humanity; we should not distort it.

A. P. J. Abdul Kalam

Non viral vectors: the objectives of nanotech studies applied to gene transfer

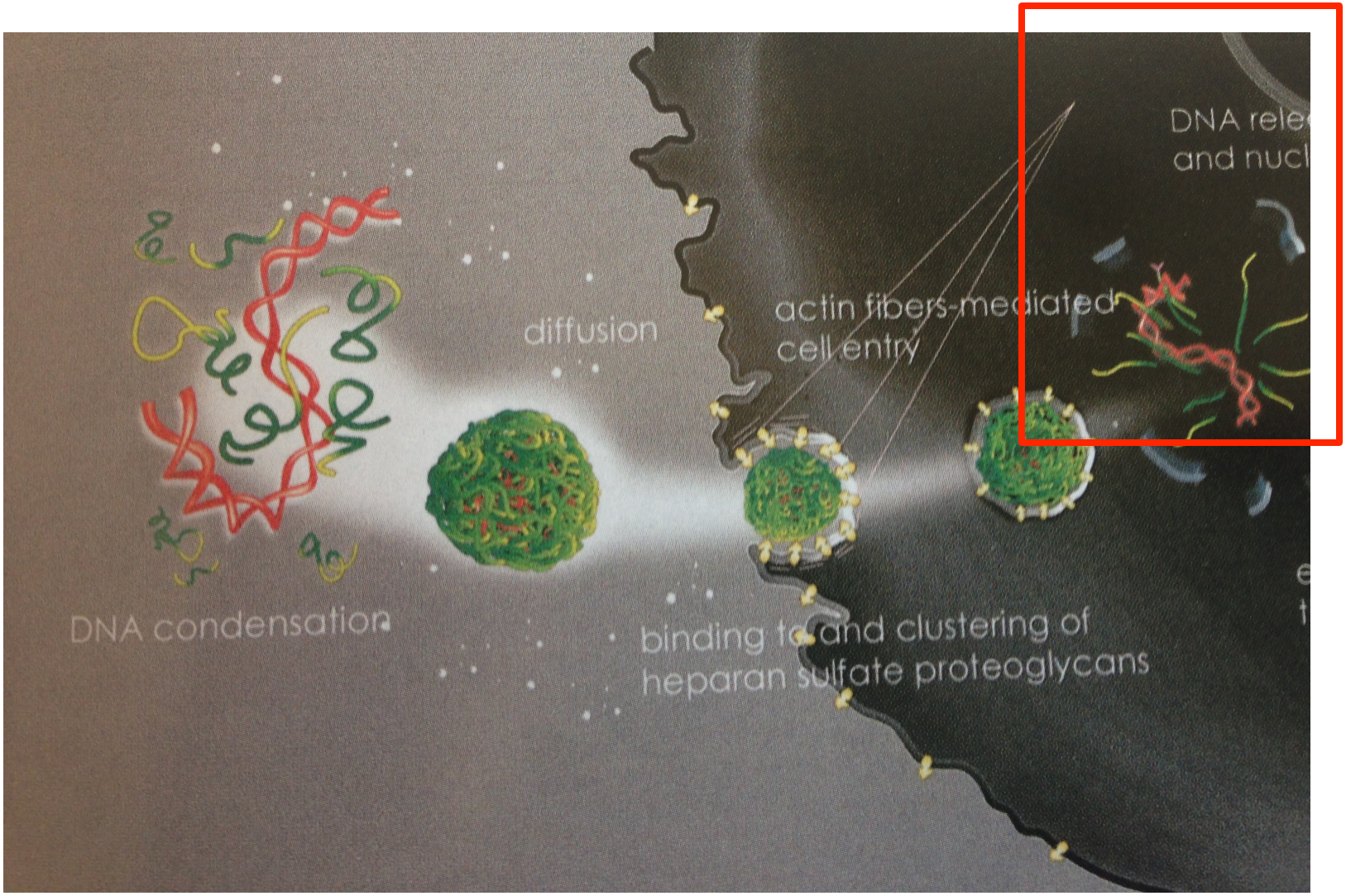

Nuclear targeting- inserting DTS (DNA nuclear Targeting Sequences) in the DNA

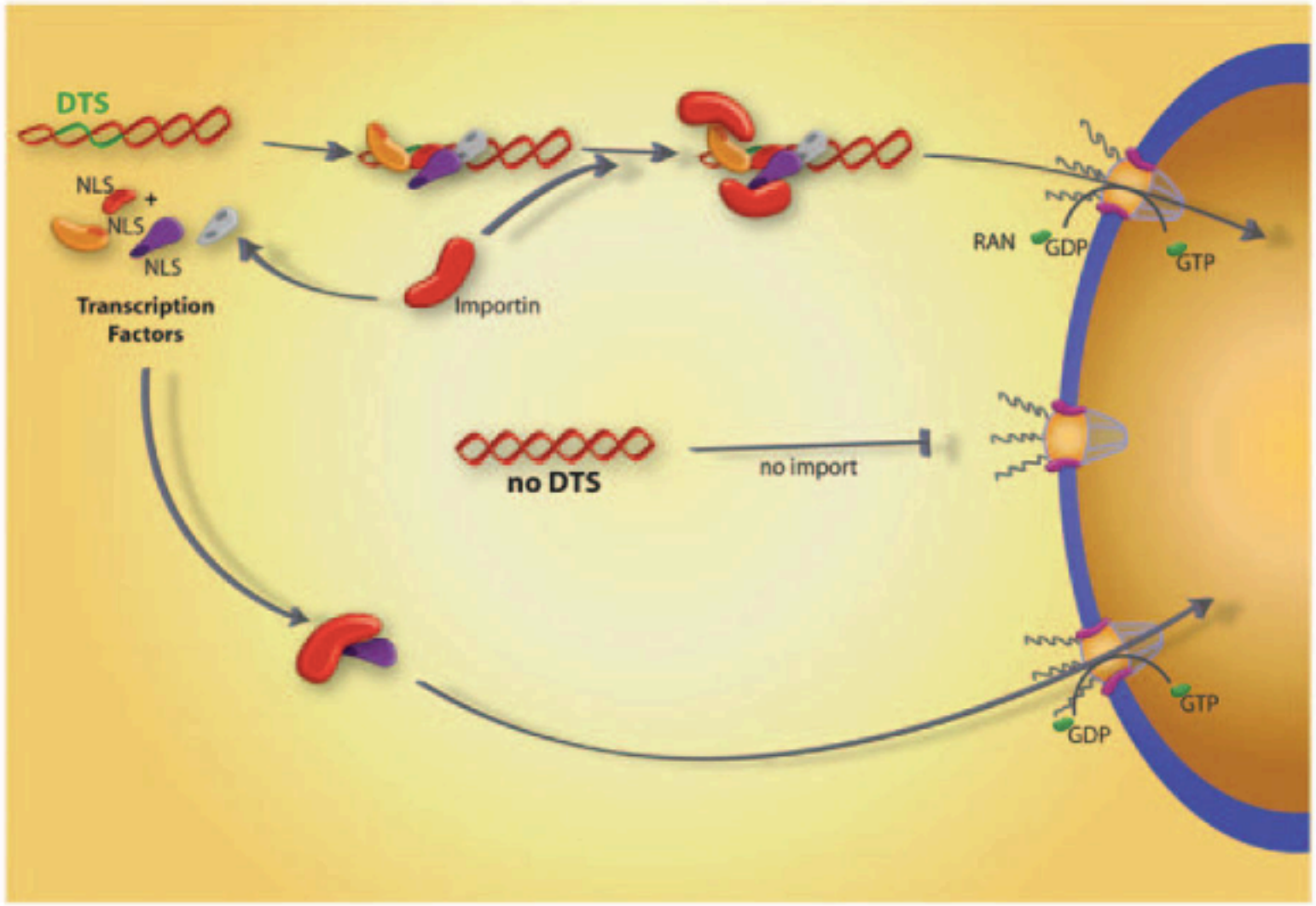

Gene therapy 2010 Lam and Dean

Cell specific nuclear targeting: DTS of smooth muscle γ-actin promoter

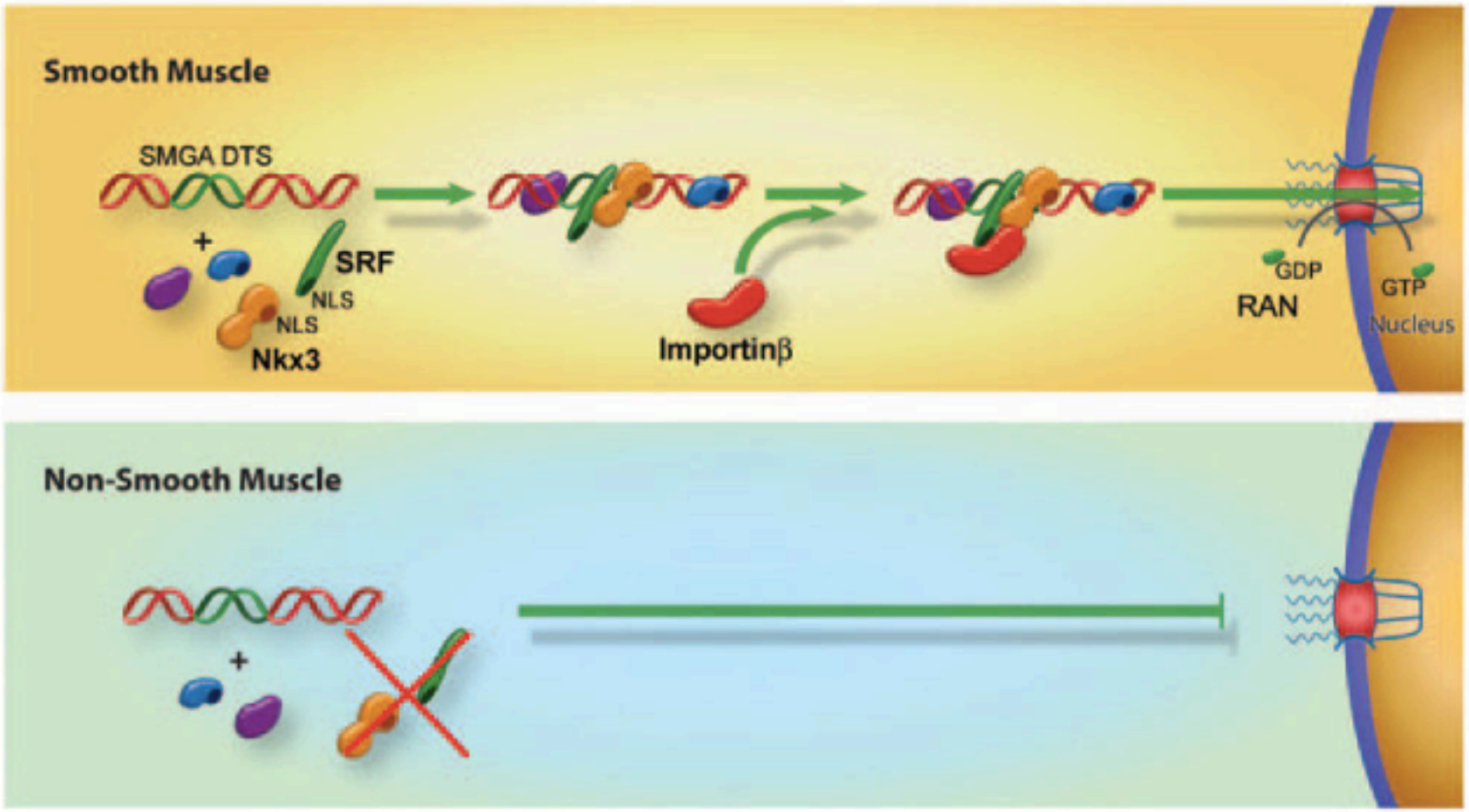

Gene therapy 2010 Lam and Dean

Addition of a nuclear localization signal-peptide

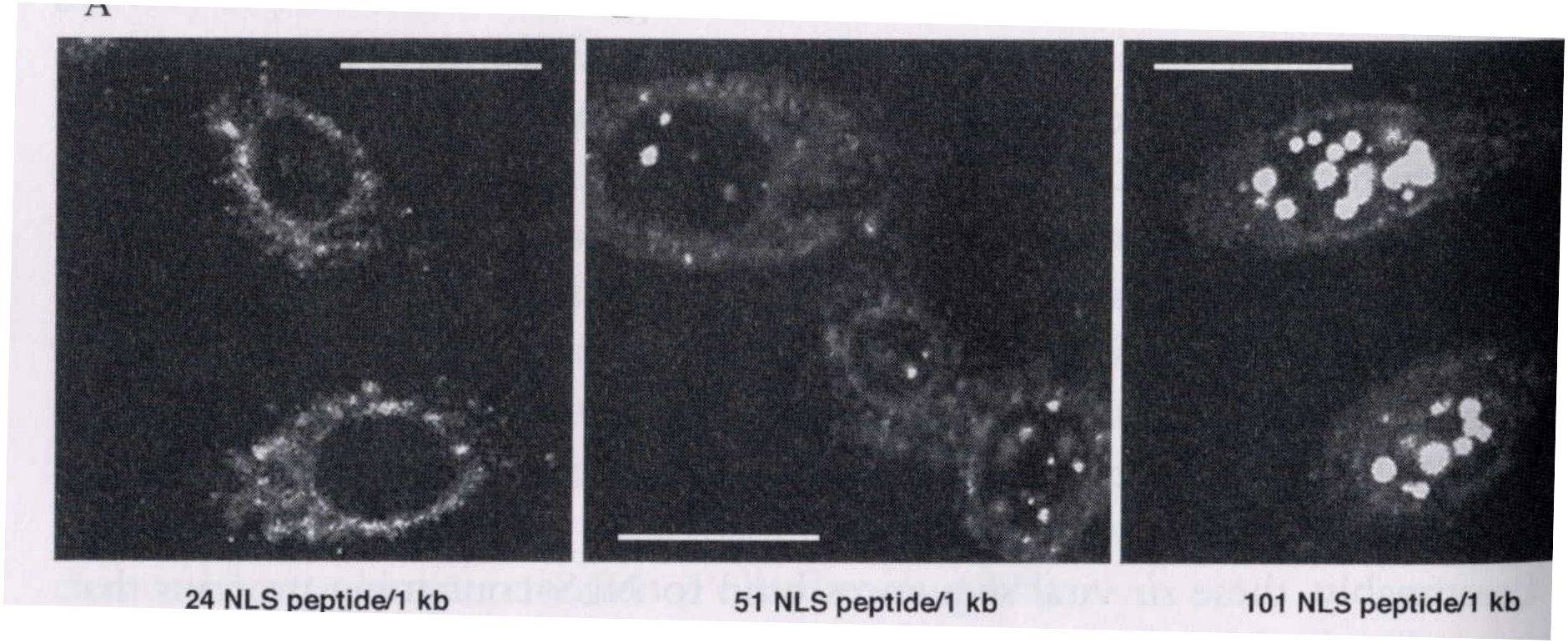

Bottom up

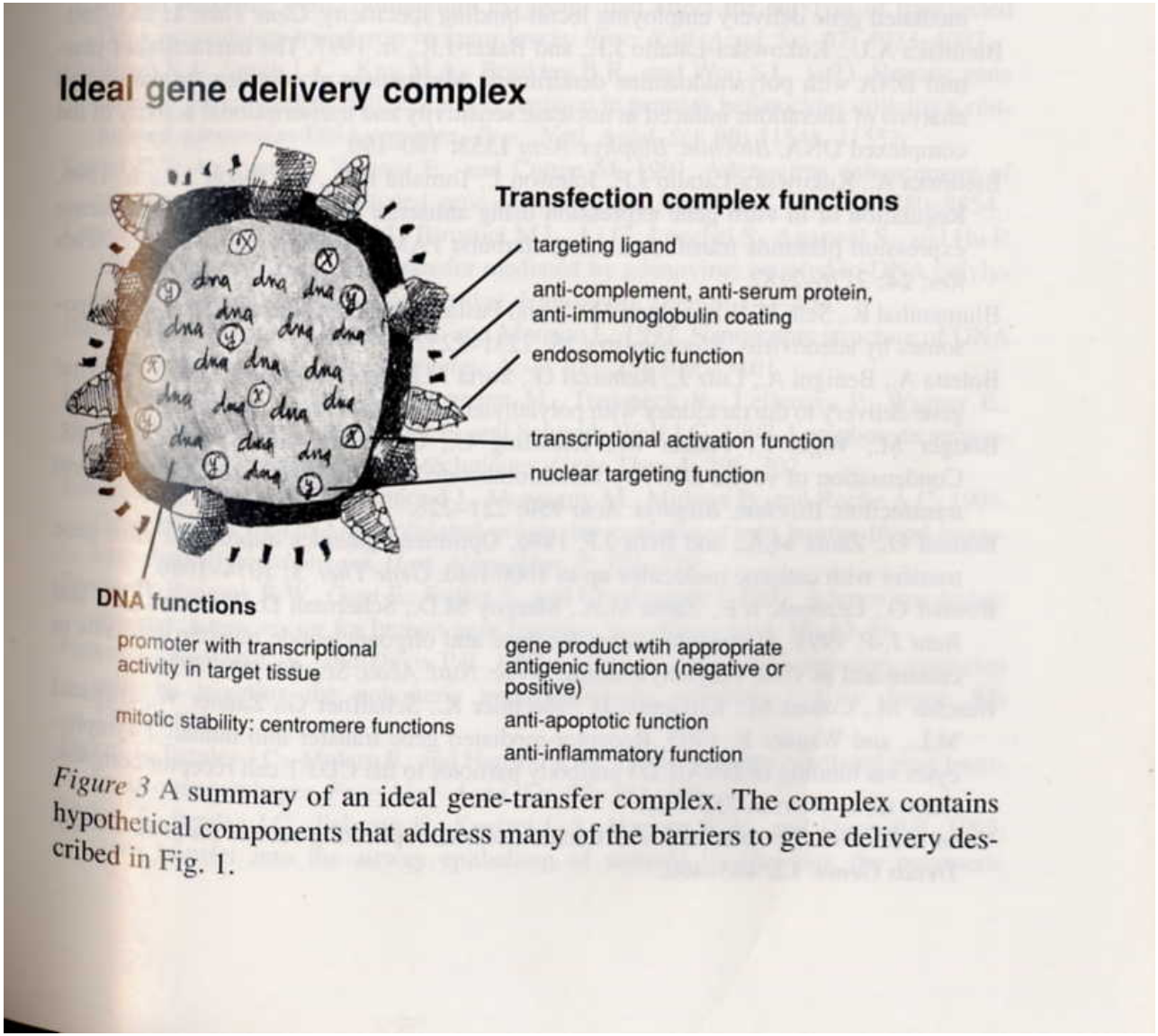

Figure 3 A summary of an ideal gene-transfer complex. The complex contains hypothetical components that address many of the barriers to gene delivery described in Fig. 1.

Viral *offer*

Table 3-2. Examples of viral entry functions

Entry function	Virus	Viral domain, mechanism
Packaging of genome	Adenovirus, Retroviruses	Mu peptide, core particle, gag proteins
Binding to cell surface	Influenza virus	HA-1, binding to sialic acid
	Rhinoviruses	major group: ICAM, minor group: LDL-receptor
	Retroviruses	MLV: gp70-phosphate transporter HIV: gp120-CD4 of T-cells;
Internalization into the cell	Adenovirus, rhinovirus, Influenza virus, SFV	endocytosis into endosomes
	Herpes viruses, HVJ	fusion at cell surface
Release into cytoplasm	Adenovirus	endosome disruption
	Rhinovirus	formation of endosomal pore; VP-1
	Influenza virus, HIV, Sendai virus, SFV	fusion; influenza HA-2, HIV gp 41, Sendai F1, SFV E1 protein
Transfer into nucleus	Adenovirus	injection of DNA through nuclear pore
	Influenza virus	transport of RNPs into nucleus
	HIV	nuclear localization of HIV core particle
Maintenance of expression	Retroviruses	integration (integrase, LTR elements)
	Adeno-associated virus	integration (rep proteins, ITR elements)
	Herpes virus, EBV	episomal persistence (e.g. oriP, EBNA-1)

Top down

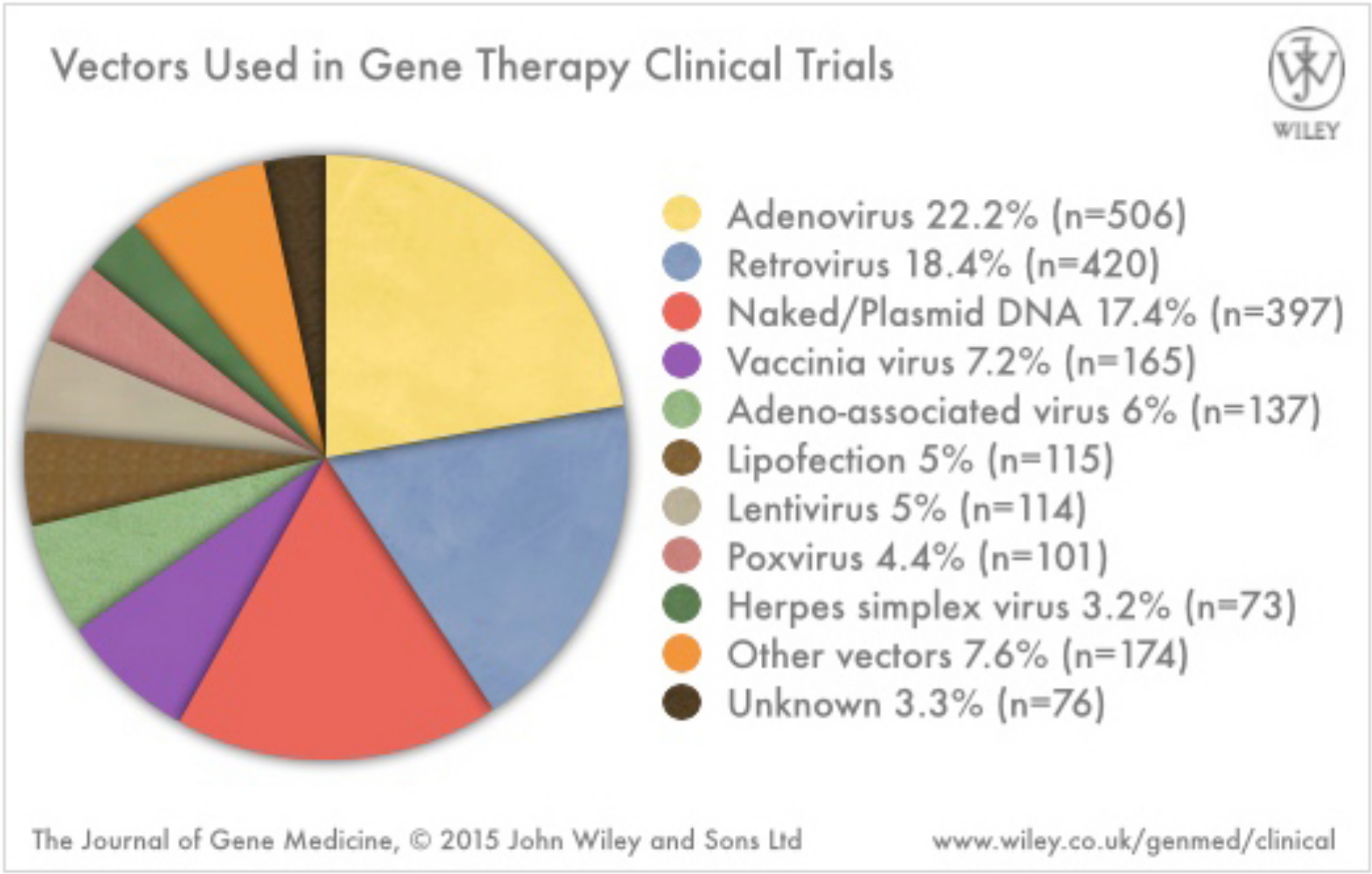
Vectors Used in Gene Therapy Clinical Trials
WILEY
Adenovirus 22.2% (n=506)
Retrovirus 18.4% (n=420)
Naked/Plasmid DNA 17.4% (n=397)
Vaccinia virus 7.2% (n=165)
Adeno-associated virus 6% (n=137)
Lipofection 5% (n=115)
Lentivirus 5% (n=114)
Poxvirus 4.4% (n=101)
Herpes simplex virus 3.2% (n=73)
Other vectors 7.6% (n=174)
Unknown 3.3% (n=76)
The Journal of Gene Medicine, © 2015 John Wiley and Sons Ltd
www.wiley.co.uk/genmed/clinical

ISI adenovirus and gene therapy 1985 -2011

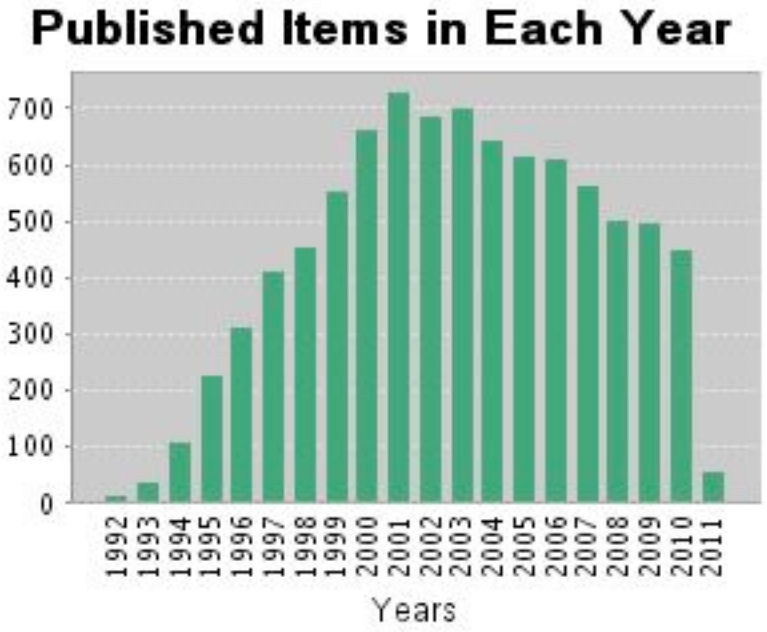

8872 papers, h index 179

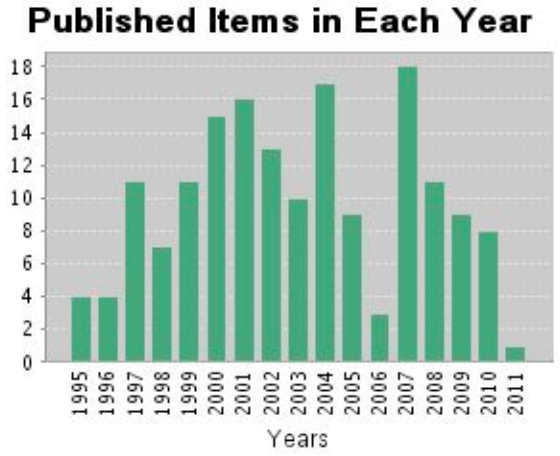

+Italy h index 36

Ad

- isolated in adenoids
- largest nonenveloped viruses
- 51 immunologically distinct human serotypes (6 species: *A* through *F*)
- cause infections ranging from respiratory disease (mainly species HAdV-B and C), and conjunctivitis (HAdV-B and D), to gastroenteritis (HAdV-F serotypes 40 and 41)
- stable to chemical or physical agents and adverse pH conditions
- spread via respiratory droplets, fecal routes as well
- Most people recover from adenovirus infections

Ad2/5

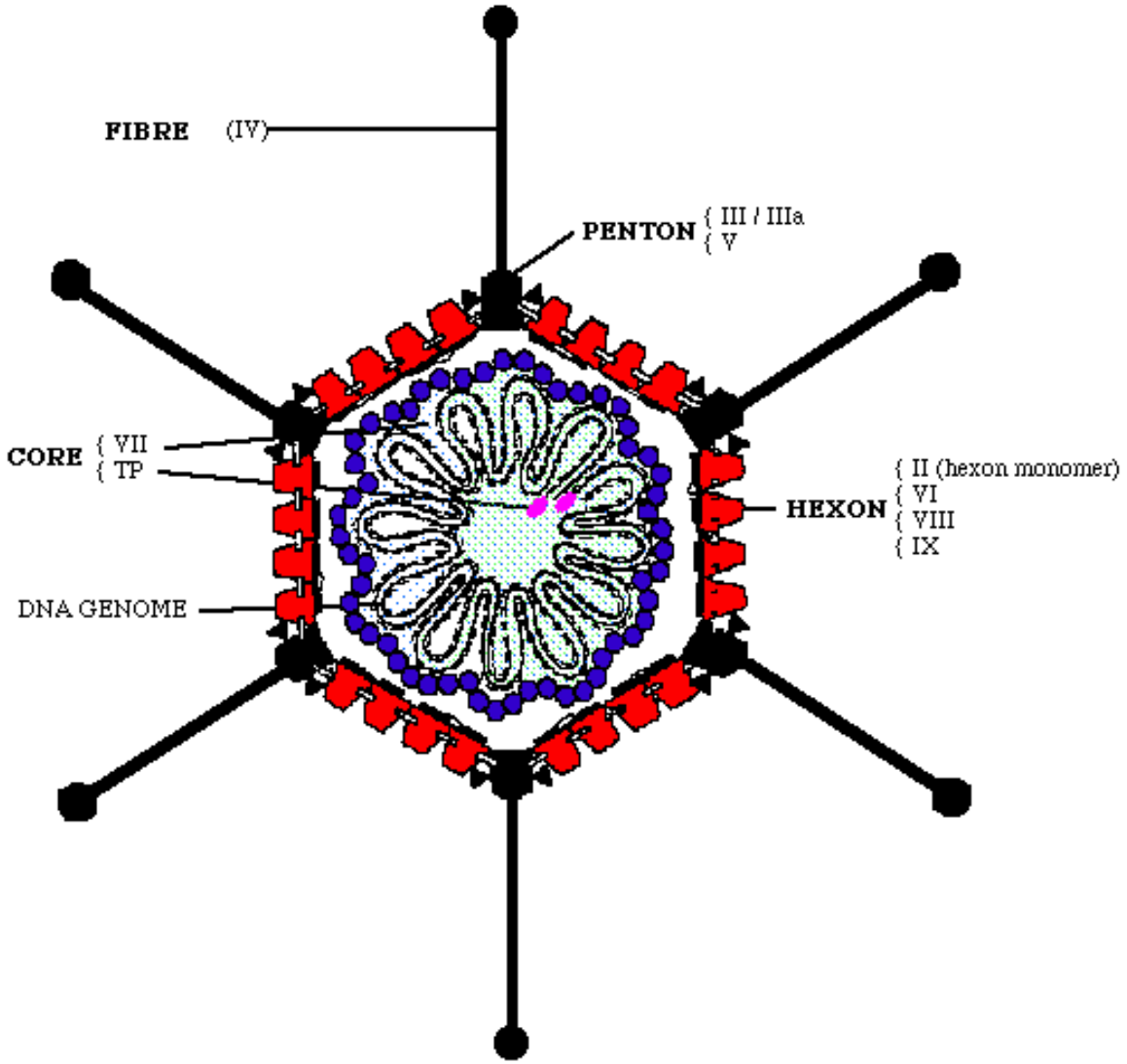
FIBRE (IV)
PENTON { III / IIIa
{ V
CORE { VII
{ TP
DNA GENOME
HEXON { II (hexon monomer)
{ VI
{ VIII
{ IX

Adeno video

http://www.youtube.com/watch?v=t7AAgXl96sA&feature=related

transmission electron microscopy (EM) where the sample is studied at cryogenic temperatures (generally liquid nitrogen temperatures).

Ad2

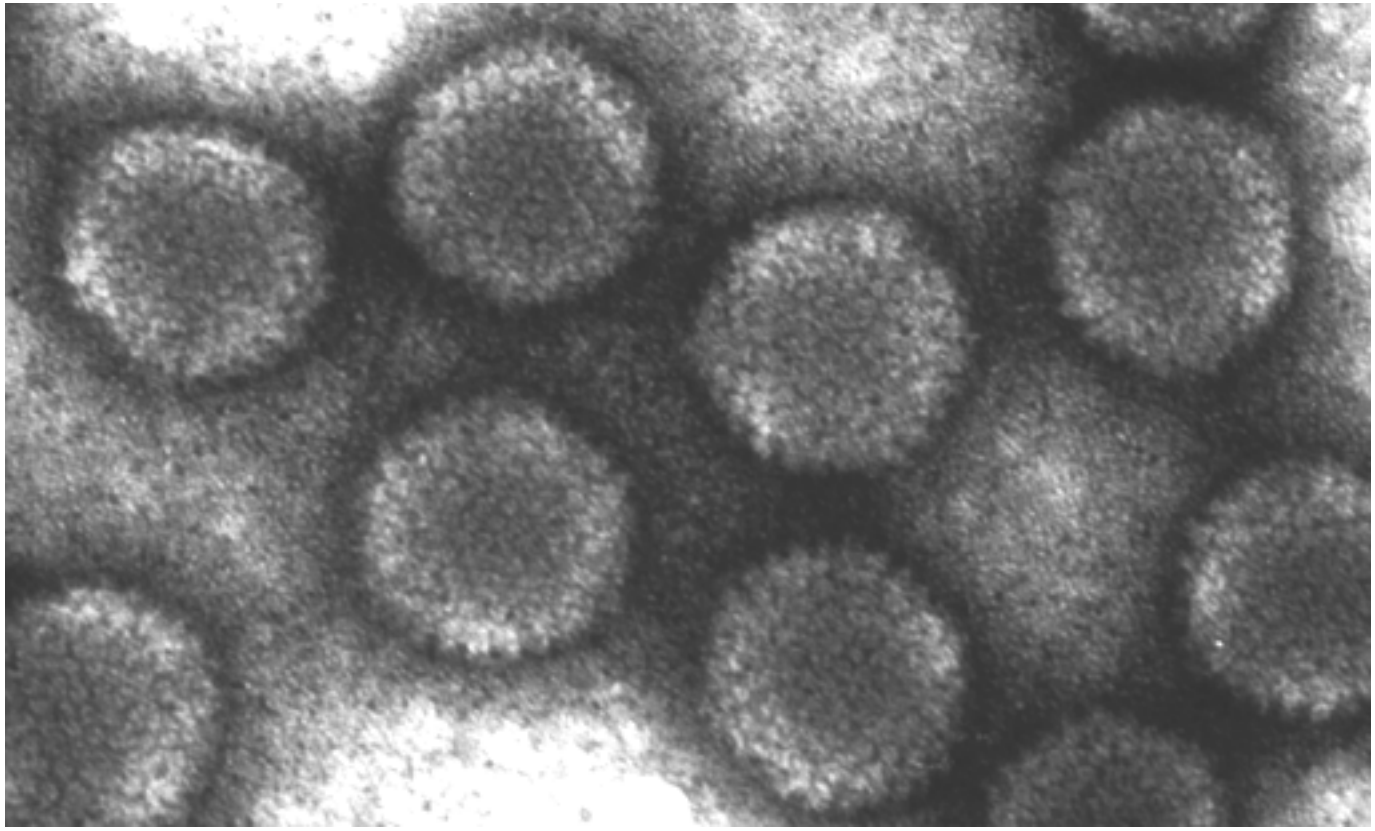

Electron micrograph of negatively stained Ad2 (source, K. Boucke). For further information see (1; 2).

(1). Valentine, R. C., and Pereira, H. G. (1965) J. Mol. Biol. 13, 13-20.
(2). Greber, U. F., et al. (1998) in Adenovirus entry into cells: A quantitative fluorescence microscopy approach, ed. W. S. M. Wold (Humana Press, Inc, Totowa, NJ USA), pp. 217-230.

Ad entry into the cell

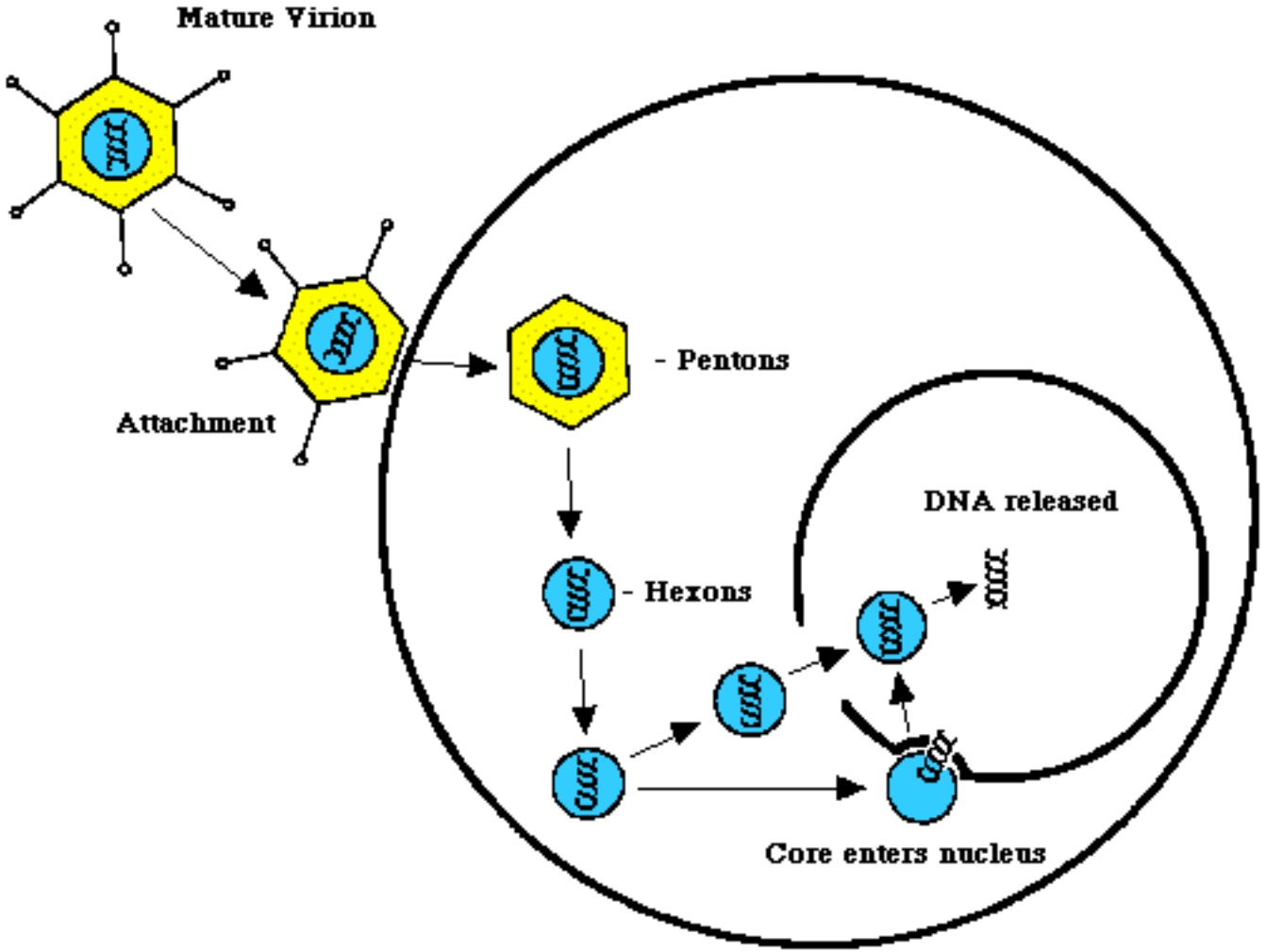

Ad-binding

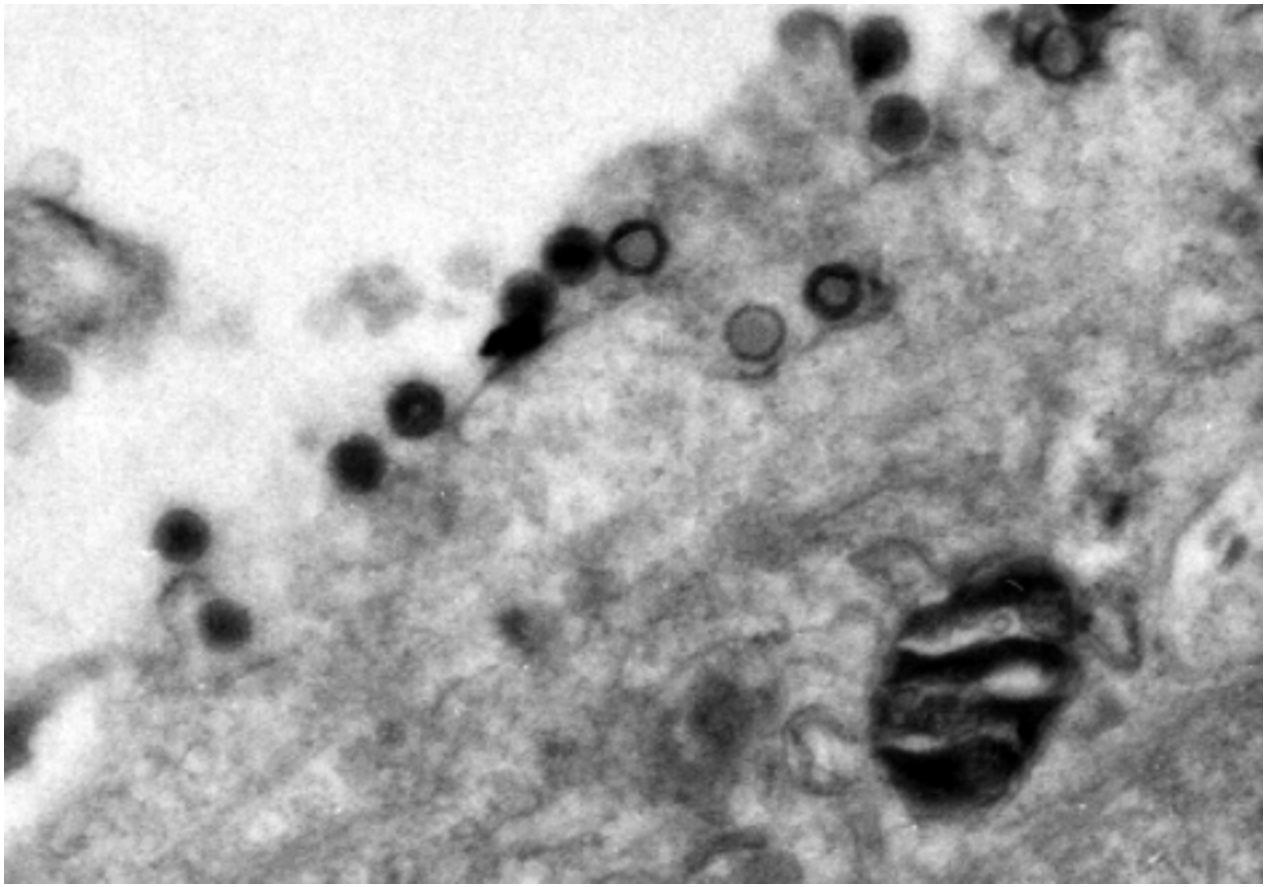

Electron micrograph of Ad2 attached to the HeLa cell surface (source, K. Boucke)

Ad-binding

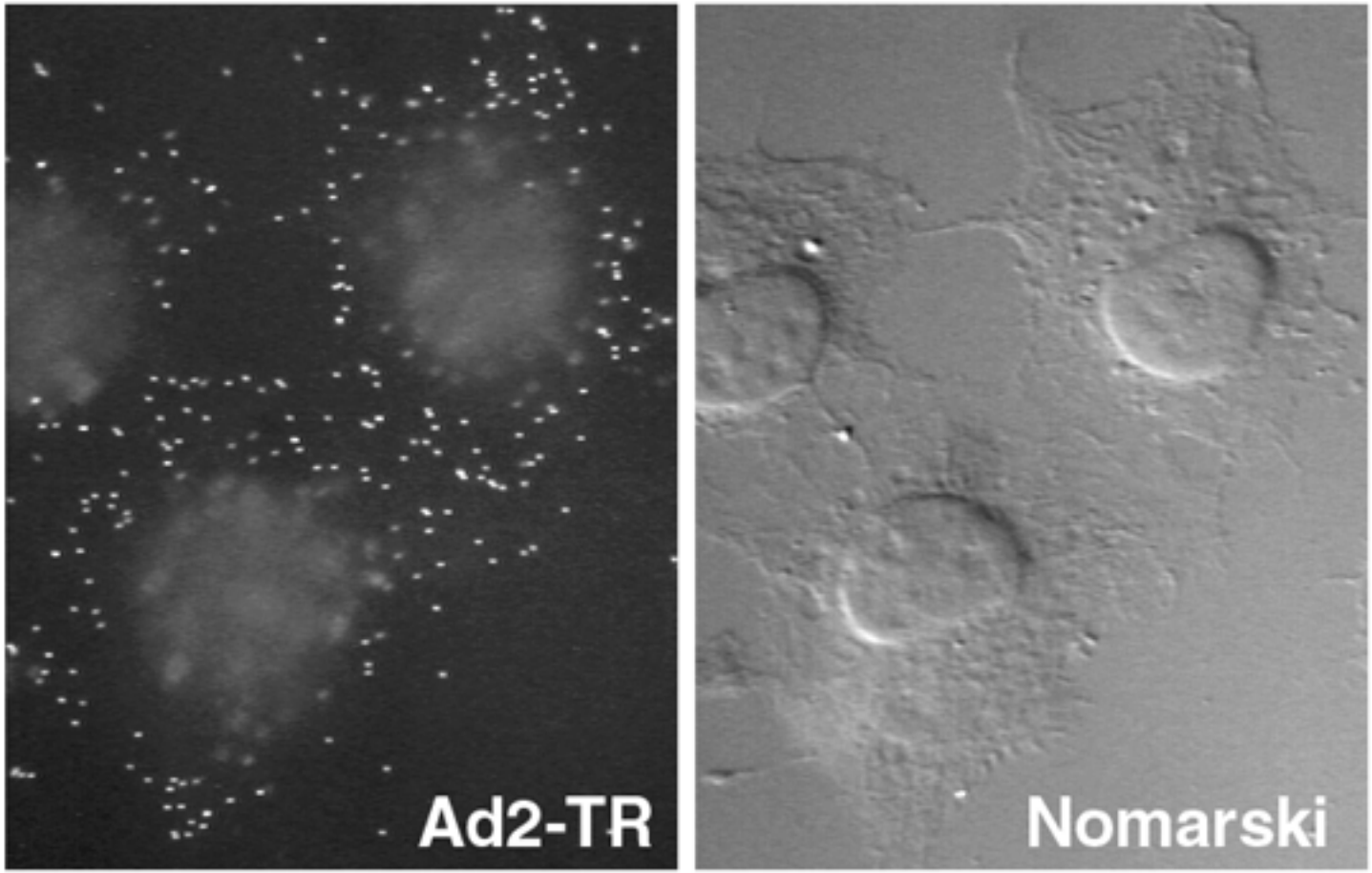

Fluorescence micrograph of texas red-labeled Ad2 bound to the surface of HeLa cells. Corresponding Nomarski image is shown on the right side (source, U. Greber).

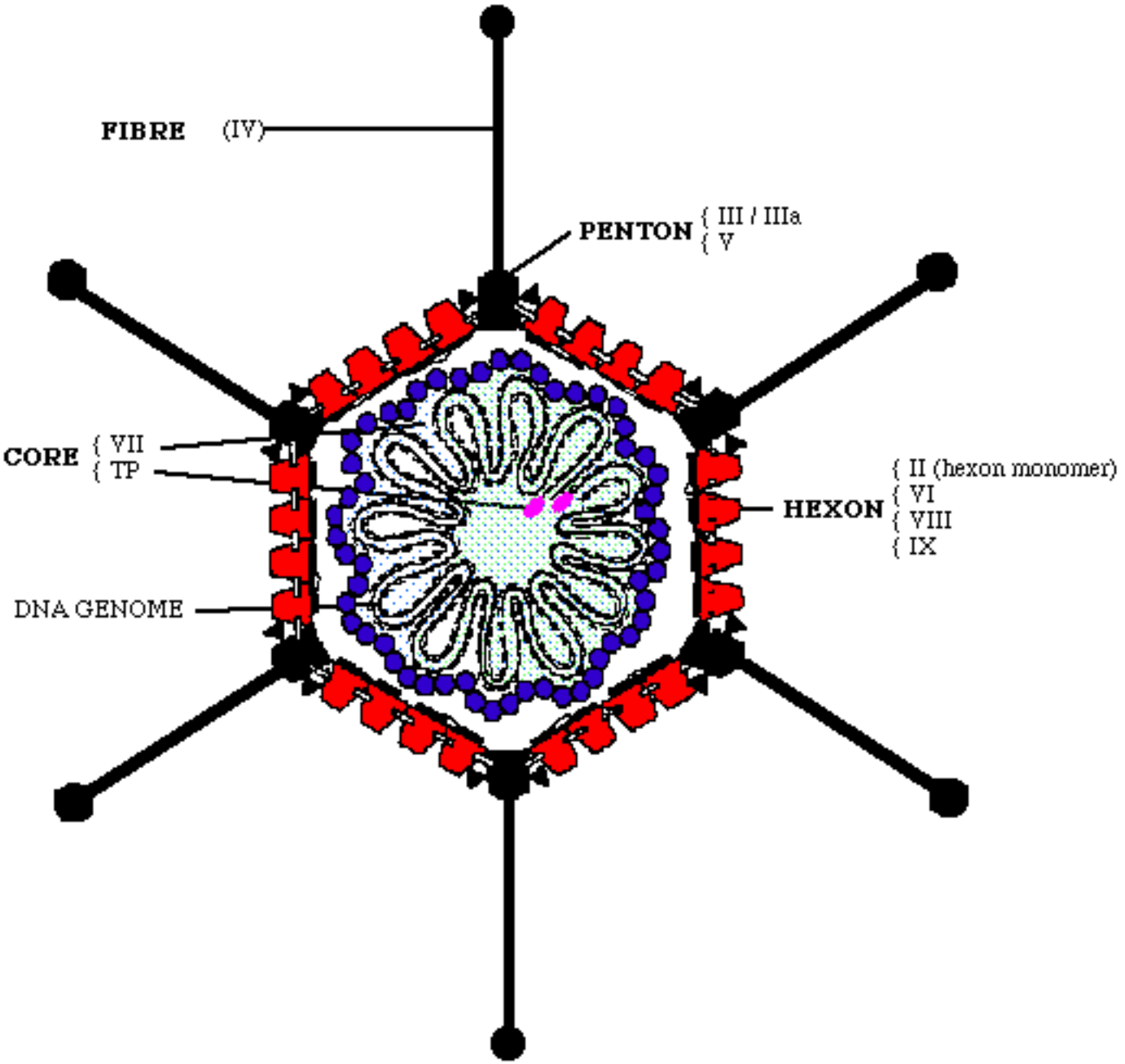
FIBRE (IV)
PENTON { III / IIIa
{ V
CORE { VII
{ TP
DNA GENOME
HEXON { II (hexon monomer)
{ VI
{ VIII
{ IX

Ad entry into cells

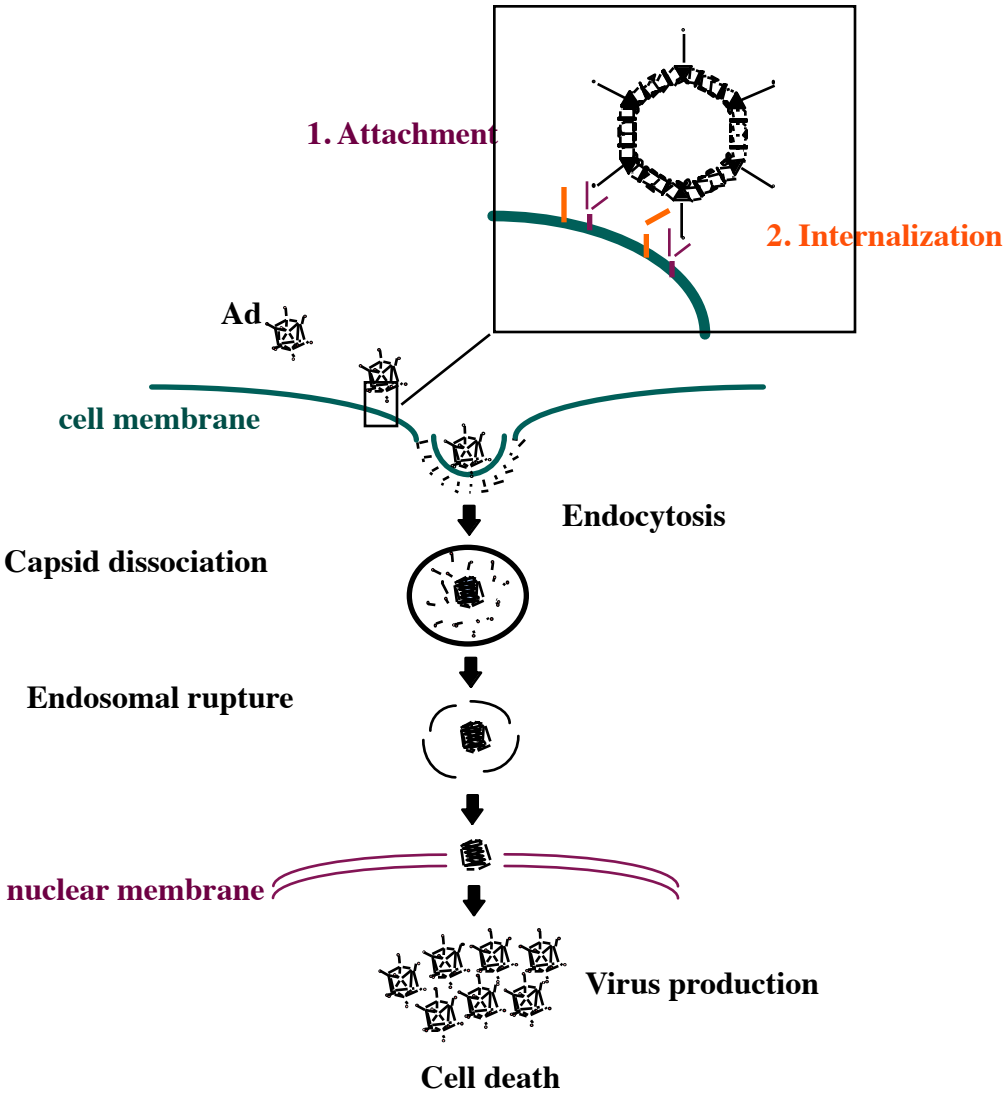

Fibre

(A) Fiber **trimers** (green) protrude from each penton complex (yellow) of the icosahedral capsid of adenovirus. The fiber trimer comprises N-terminal tails (thin tubes), a central shaft, and a globular knob (ovals). The third -repeat of the shaft is indicated by a red arrow. (B) Critical features of the fiber are shown in the crystal structure of Ad 2 fiber. beta-strands of the fiber knob are lettered from A to J, according to the nomenclature of Xia et al. 97. The CAR binding site, which is made up mostly by the AB loop (ball and stick), lies along the side of the fiber knob trimer. **Locations of some mutations that abolish CAR binding are indicated by arrows**. The HI loop is shown in magenta. The final four -repeats of the fiber shaft (18–21) are shown with Roman numerals. This image was made using Molscript98. (Features were omitted in blue model for clarity).

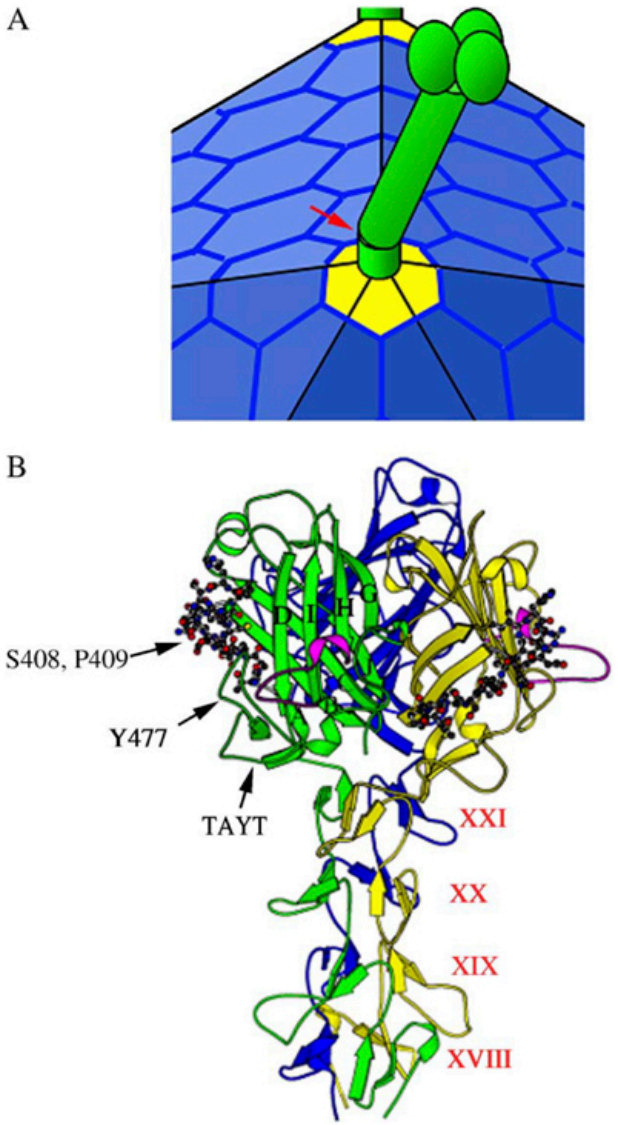

Ad-Hexon

Coagulation factor FX binds to the Ad5 hexon, not fiber, via an interaction between the FX Gla domain and hypervariable regions of the hexon surface. Liver infection by the FX-Ad5 complex is mediated through a heparin-binding exosite in the FX serine protease domain. This study reveals an unanticipated function for hexon in mediating liver gene transfer invivo.

Cell 2008 A. Baker

Ad-Hexon

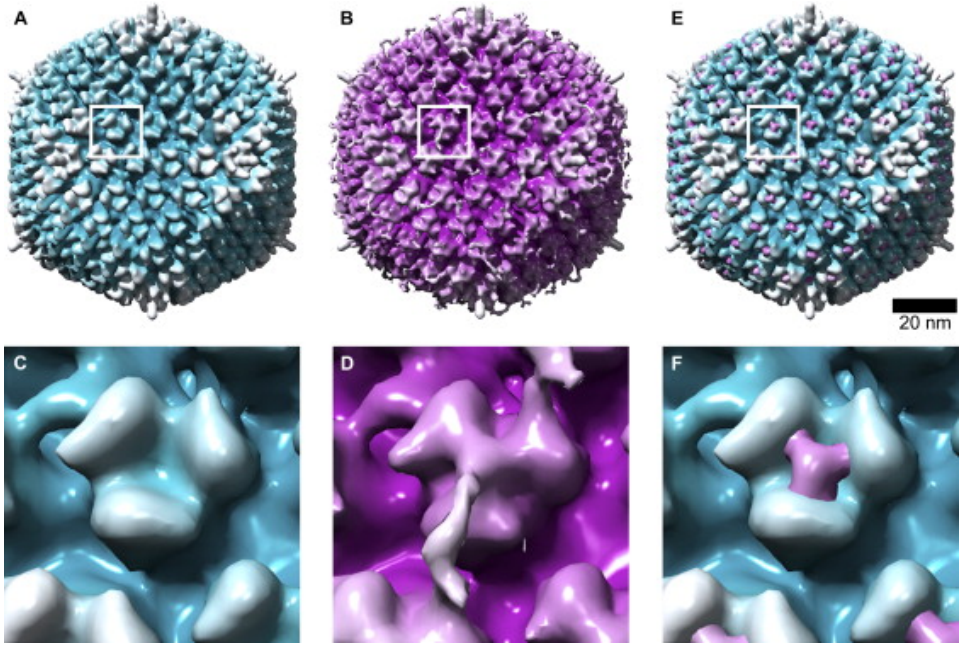

Azzurro esone
Violetto FX

(A and B) Three-dimensional reconstructions of uncomplexed Ad5 (A) and FX-Ad5 complex (B) surface contoured to include density above the mean plus one standard deviation of total map density.

(C and D) Closeup view of an uncomplexed (C) and FX-complexed (D) hexon.

(E) Overlaid reconstructions of uncomplexed Ad5 (blue) and FX-Ad5 complex (purple). The scale bar represents 20 nm. The surface threshold level of the FX-Ad5 structure is raised to highlight the point of contact between FX and Ad5 hexon.

(F) Closeup view of FX-labeled hexon.

Cell 2008 A. Baker

Ad-Hexon

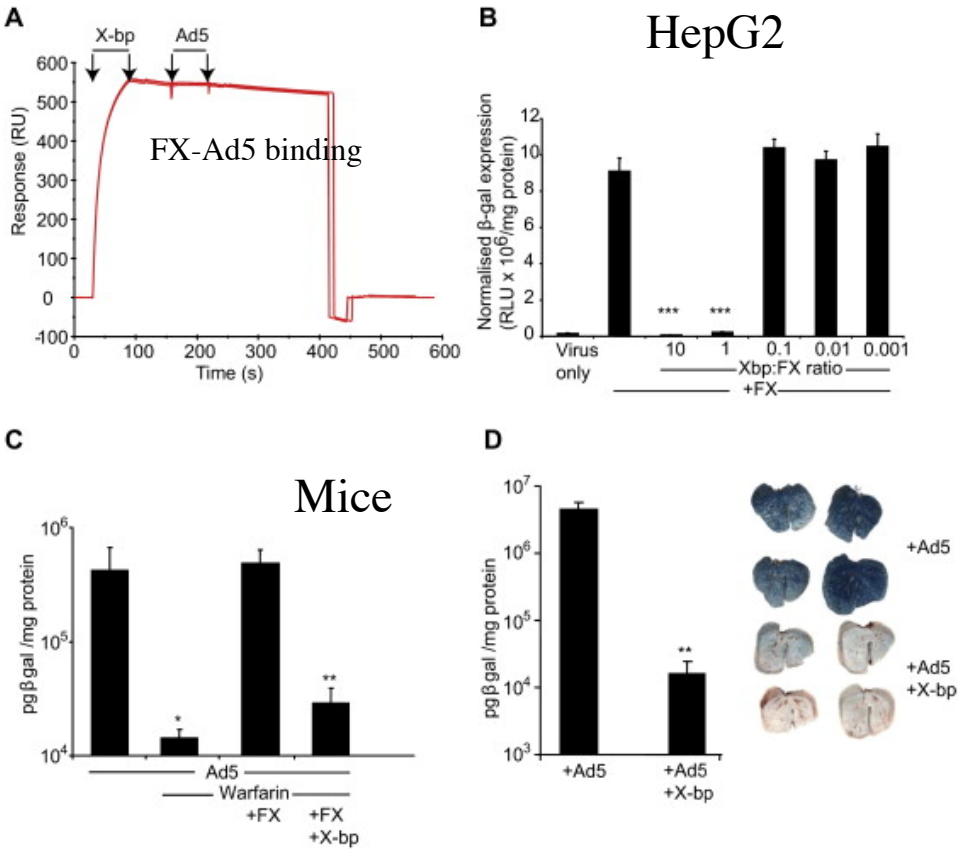

Figure 6. Pharmacological Blockade of Ad5 Binding to FX by **Snake Venom Protein X-bp** Blocks Liver Transduction In Vivo

(A) Subtracted SPR sensorgram (FX-FXI) shows X-bp binding with high affinity (increase in RU following X-bp injection) and ablates subsequent FX-Ad5 binding (no change in RU following Ad5 injection). Arrows indicate the start and end of reagent injection.

(B) HepG2 cells were exposed to AdKO1 in the presence of FX alone or FX preincubated with X-bp at different FX:X-bp molar ratios (as shown). ***p < 0.0001 versus no X-bp. Error bars represent SEM.

(C) MF-1 mice were pretreated with control peanut oil or warfarin and injected with 4 × 1011 VP/mouse Ad5 with or without preinjection of FX alone or preincubated with three-fold molar excess of X-bp. *p = 0.006; **p = 0.0002. Error bars represent SEM.

(D) MF-1 mice (nonwarfarinized) were injected with X-bp 30 min prior to Ad5 injection. Forty-eight hours later liver gene transfer was quantified by ELISA (bar graph) and visualized by staining for β-galactosidase (pictures). (**p = 0.0002). Error bars represent SEM.

Warfarin: blocks reductase -> blocks vitK-> blocks FX
Xbp: binds and blocks directly FX

Cell 2008 A. Baker